Journal of Solid State Chemistry 183 (2010) 1761–1766

Contents lists available at ScienceDirect

Journal of Solid State Chemistry

journal homepage: www.elsevier.com/locate/jssc

Polymer-directed synthesis and magnetic property of nanoparticles-assembled $BiFeO_3$ microrods

Lei Zhang [a], Xiao-Feng Cao [a], Ying-Li Ma [a], Xue-Tai Chen [a,*], Zi-Ling Xue [b]

[a] State Key Laboratory of Coordination Chemistry, Nanjing National Laboratory of Microstructures, School of Chemistry and Chemical Engineering, Nanjing University, Nanjing 210093, PR China

[b] Department of Chemistry, The University of Tennessee, Knoxville, TN 37996-1600, USA

ARTICLE INFO

Article history:
Received 9 March 2010
Received in revised form
21 May 2010
Accepted 22 May 2010
Available online 2 June 2010

Keywords:
Oxide materials
Microstructure
Magnetic measurements

ABSTRACT

Nanoparticles-assembled $BiFeO_3$ microrods were successfully prepared via a polymer-directed solvothermal route. The phase and morphology of the products were characterized by powder X-ray diffraction (XRD), energy dispersive spectrometry (EDS), inductively coupled plasma atomic emission spectroscopy (ICP-AES), FT-IR spectroscopy and scanning electron microscopy (SEM). Experiments indicated that the linking effect originated from the interactions between polymer molecules could direct the self-assembly of building blocks into one-dimensional nanoparticles-assembled $BiFeO_3$ microrods. Some factors influencing the morphologies of the products were systematically investigated and a possible mechanism of the formation of the microrods was suggested. Moreover, the magnetic properties of the products were studied.

1. Introduction

The shape- and size-controlled synthesis of functional nanomaterials has been receiving considerable attention because the morphology, dimensionality and size of the materials generally have great effects on their physical and chemical properties [1–3]. In this respect, various methods have already been designed and much significant progress has been made [4–7]. However, preparation of technologically useful nanoparticles-based materials and their practical applications depend not only on the quality (e.g., size and shape), but also on their spatial orientation and arrangement. The self-assembly of functionalized nanoparticles affords a new route to control structural, electronic and optical properties by tuning the core sizes of the particles and the chemistry of the attached ligands [8–10]. Nevertheless, fabrication of hierarchal structures based on the self-assembly of nanoparticles usually needs a multistep process and most of the studies are focused on the metals, metal chalcogenides and binary metal oxides [11–15]. It is still a challenge to develop one-step synthetic route to construct such nanoparticles-assembled structures of ternary metal oxides.

Multiferroics, showing the coexistence of magnetic and ferroelectric orders in a certain range of temperature, have attracted a great deal of attention due to the fascinating fundamental physics and their potential applications in information storage, spintronic devices and sensors [16–20]. Perovskite-type $BiFeO_3$ (BFO) is one of the representative multiferroic materials that exhibit a relatively high Neel temperature ($T_N \sim 375\ ^\circ C$) and Curie temperature ($T_C \sim 830\ ^\circ C$). In addition to the potential magnetoelectric applications, BFO has also wide applications as photocatalytic materials due to its small bandgap [16]. Usually, BFO nanomaterials were prepared using a variety of synthetic methods, such as solid-state reaction [21], sol–gel technique [22–24] and combustion [25]. For example, Gao et al. [26] have successfully prepared BFO nanoparticles ranging from 80 to 120 nm by a simple sol–gel method. Fang and co-workers [27] first reported one-dimensional single-crystalline nanostructures of $BiFeO_3$ and $Bi_2Fe_4O_9$ synthesized by a template-free route via soft chemistry with the precursor in a thin-film form.

Recently, hydrothermal and solvothermal routes offer the possibilities to obtain phase-pure BFO samples [28–30], which usually require high temperatures, long reaction times and high concentration of alkalis to prepare. It is an interesting and urgent work to design a facile, rapid and economical pathway to prepare one-dimensional BFO materials. Herein, we report the successful synthesis of one-dimensional nanoparticles-assembled BFO microrods via an one-step polymer-directed solvothermal route. Compared with Fang's work, our work presented some distinct differences: firstly, pure phase BFO materials were prepared by an one-step solvothermal route and post-treatment is needless; secondly, the presence of polymer can direct BFO nanoparticles to novel rod-like assemblies; moreover, the magnetic properties of such BFO microrods and nanoparticles were studied.

* Corresponding author. Fax: +86 25 83314502.
E-mail address: xtchen@netra.nju.edu.cn (X.-T. Chen).

0022-4596/$ - see front matter © 2010 Elsevier Inc. All rights reserved.
doi:10.1016/j.jssc.2010.05.029

2. Experimental section

All reagents were purchased from Shanghai Chemical Company and used without further purification. In a typical preparation procedure, $Bi(NO_3)_3 \cdot 5H_2O$ (0.001 mol) and $Fe(NO_3)_3 \cdot 9H_2O$ (0.001 mol) were dissolved in 1 mL of HNO_3 (65%, mass fraction). Then, 25 mL of absolutely ethanol containing 1 g of PVP was slowly dropped into the above solution. Finally, 1.2 g of NaOH was added. The as-obtained solution was stirred for 10 min and transferred into stainless-steel autoclave with a Teflon liner of 40 mL capacity. After treating the mixture at 180 °C for 6 h, it was cooled to room temperature naturally. The product was collected, washed with deionized water and absolute ethanol, and dried in vacuum at 60 °C for 6 h with a yield of 90%.

The products were characterized by X-ray powder diffraction (XRD) with a Shimadzu XRD-6000 powder X-ray diffractometer with Cu $K\alpha$ radiation (λ=1.5418 Å), recorded with 2θ ranging from 15° to 70°. SEM images and EDS of the products were obtained on field emission scanning electron microanalysers (Hitachi S-4800), employing the accelerating voltage of 5 or 20 kV. The Bi/Fe molar ratio of the as-synthesized product was analyzed by inductively coupled plasma atomic emission spectroscopy (J-A1100 from Jarrell-Ash Corp). FT-IR spectra were recorded for KBr-diluted samples using a Nicolet Magna 750 IR spectrometer at wavenumbers 400–4000 cm^{-1}. The magnetic properties of the products were obtained on superconducting quantum interference device (SQUID) magnetometer (Quantum Design).

3. Results and discussion

Fig. 1a depicts the XRD pattern of the product prepared at 180 °C for 6 h. All the reflection peaks could be indexed to a pure rhombohedral phase BFO with calculated lattice constants of a=5.57 Å and c=6.92 Å, which are in good agreement with the literature values (JCPDS file Card No. 14-0181). No other impurity peak is detected. Additional evidence of the formation of $BiFeO_3$ came from energy dispersion X-ray analysis. Fig. 1b shows the energy dispersion X-ray spectrum (EDS) of the as-prepared product. The peaks of Bi, Fe and O can be easily found. Besides, the C, Cu, Au peaks in the spectrum can be attributed to PVP molecule adsorbed by the sample, the substrate and the gold sputtering, respectively. ICP-AES was also used to determine the atomic ratio of Bi/Fe in the product. The experimental result shows that the Bi/Fe molar ratio of $BiFeO_3$ powders is 1.006:1, which is very close to the theoretic value of 1:1.

The structure and morphology of the product were also investigated by SEM. As shown in Fig. 2, the as-prepared product is composed of nanoparticles-assembled $BiFeO_3$ microrods with the diameter in ~1 μm and the length from 10 to 20 μm. A high magnification SEM image of an individual rod-like structure reveals that the microrod is comprised of many cube-like nanoparticles with the diameters ranging from 50 to 150 nm (Fig. 2c and d). These building blocks are arranged along a certain direction. A careful observation of these linear aggregations reveals that the primary particles are not fused with each other well since the boundaries of the particle connections are observable.

To investigate the effects of other reaction parameters such as the amount of NaOH, PVP and reaction temperature, controlled experiments were conducted to compare these effects. It has been found that the phase and morphology of the final product is strongly dependent on the amount of NaOH. When the amount of NaOH was controlled at 0.6 g, while other experimental conditions were kept unchanged, the product was comprised of

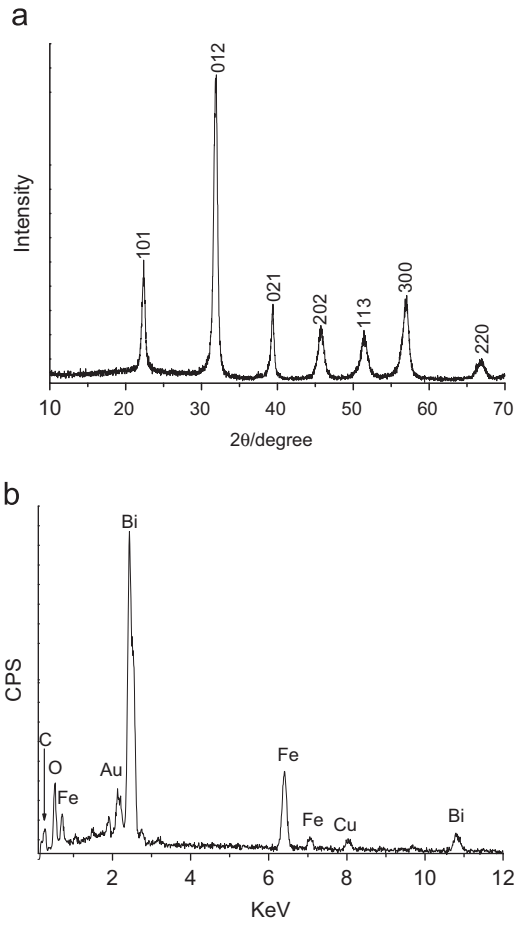

Fig. 1. (a) XRD pattern and (b) EDS spectrum of the product prepared with 1.0 g of PVP at 180 °C for 6 h.

flower-like microstructures (see Supplementary Content, Fig. S1a). The corresponding XRD pattern shown in Fig. S2a (see Supplementary Content) indicated that the sample was a mixed phase of monoclinic Bi_2O_3 (JCPDS file Card No. 76-1730), tetragonal Fe_2O_3 (JCPDS file Card No. 15-0615) and rhombohedral phase $BiFeO_3$ (JCPDS file Card No. 14-0181). If the amount of NaOH was controlled at 0.9 g, rhombohedral phase $BiFeO_3$ microspheres and nanoparticles were obtained (see Supplementary Content, Figs. S1b and S2b). Increasing the amount of NaOH to 1.2 g, nanoparticles-assembled $BiFeO_3$ microrods were the exclusive product (Figs. 1a and 2). Further increasing the amount of NaOH to 1.5 g, nanosheets and irregular nanoparticles coexisted in the final product (see Supplementary Content, Fig. S1c). The XRD pattern indicated that the present sample was also a mixed phase (see Supplementary Content, Fig. S2c). The above experiments demonstrate that the appropriate amount of NaOH is a key parameter in the formation of nanoparticles-assembled BFO microrods.

Reaction temperature is another important factor affecting the chemical reaction. The variation of reaction temperature greatly changes the product morphology and phase. When the reaction was carried out at 200 °C, some nanoparticles-assembled BFO microrods were obtained (see Supplementary Content, Figs. S3a and S4a). When the temperature was decreased to 150 °C, the product was a mixed phase (monoclinic Bi_2O_3, tetragonal Fe_2O_3 and rhombohedral phase $BiFeO_3$) and comprised of nanosheets and plates-assembled spheres (see Supplementary Content, Figs. S3b and S4b). These experiments indicate that the reaction temperature is undoubtedly indispensable for the formation of

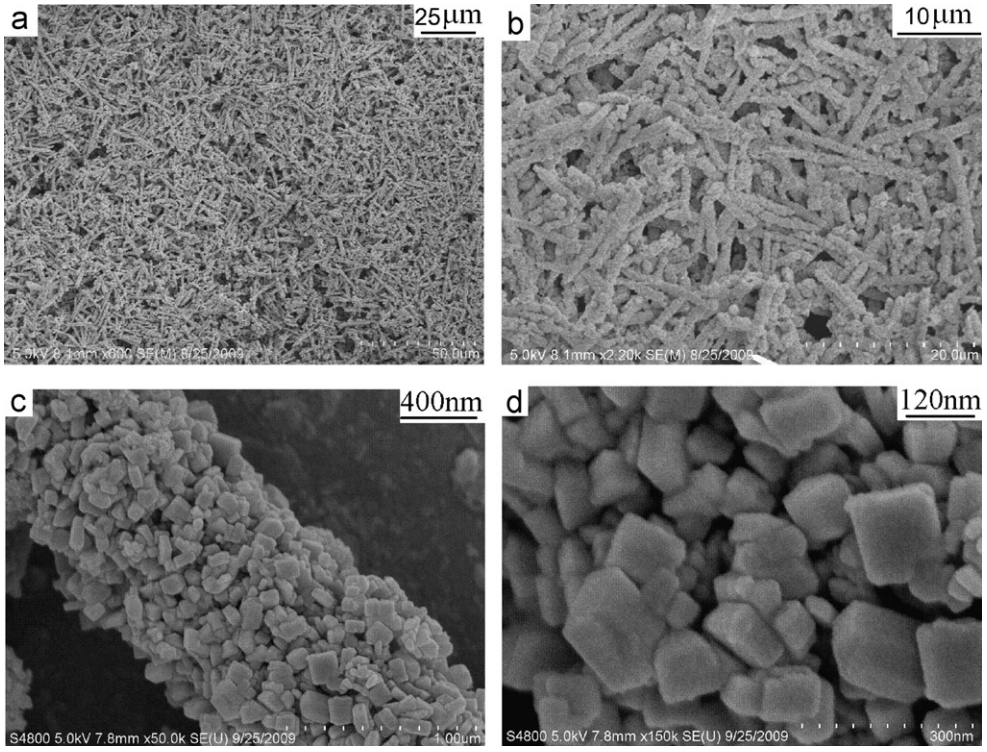

Fig. 2. SEM images of the $BiFeO_3$ sample prepared with 1.0 g of PVP at 180 °C for 6 h.

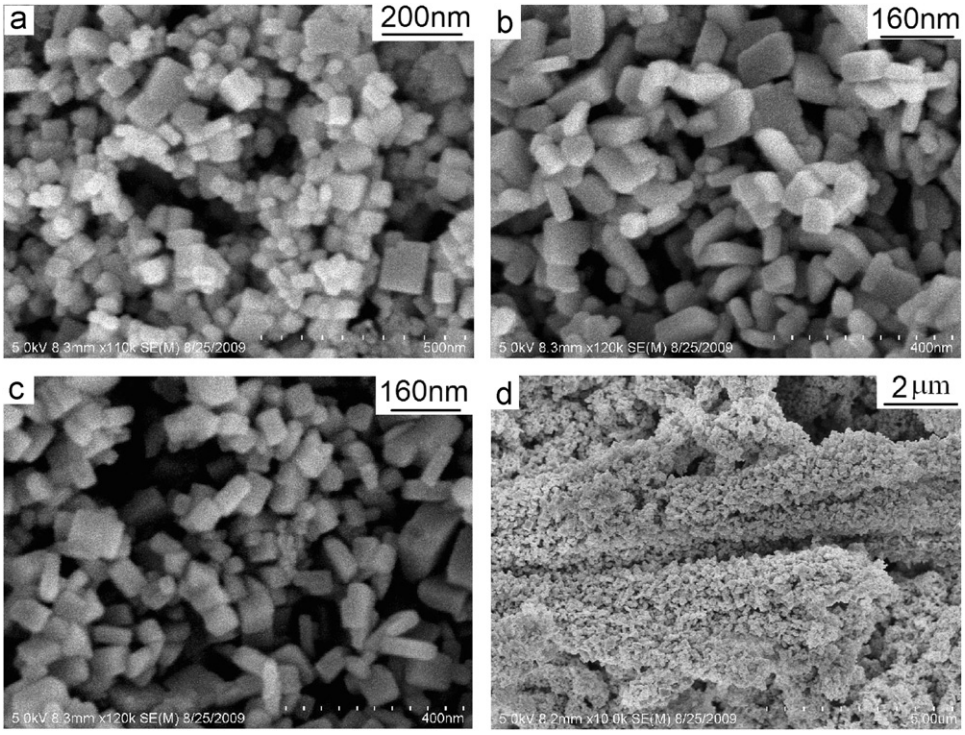

Fig. 3. SEM images of the products with different amount of PVP: (a) 0 g, (b) 0.3 g, (c) 0.7 g and (d) 1.3 g.

nanoparticles-assembled BFO microrods and 180 °C is found to be optimum.

Usually, the presence of polymer in a reaction system can efficiently control the morphology and size of nanomaterials. In the present experiment, we find that, if the amount of PVP is not more than 0.7 g, the final products are comprised of many nanoparticles (Fig. 3a–c). Increasing the amount of PVP to 1 g, nanoparticle-assembled BFO microrods are formed (Fig. 2). Further increasing to 1.3 g, such one-dimensional aggregations still exist. But, many nanocubic building blocks are simultaneously obtained (Fig. 3d). Only when the amount of PVP is more than 0.7 g can the nanoparticles-assemble BFO

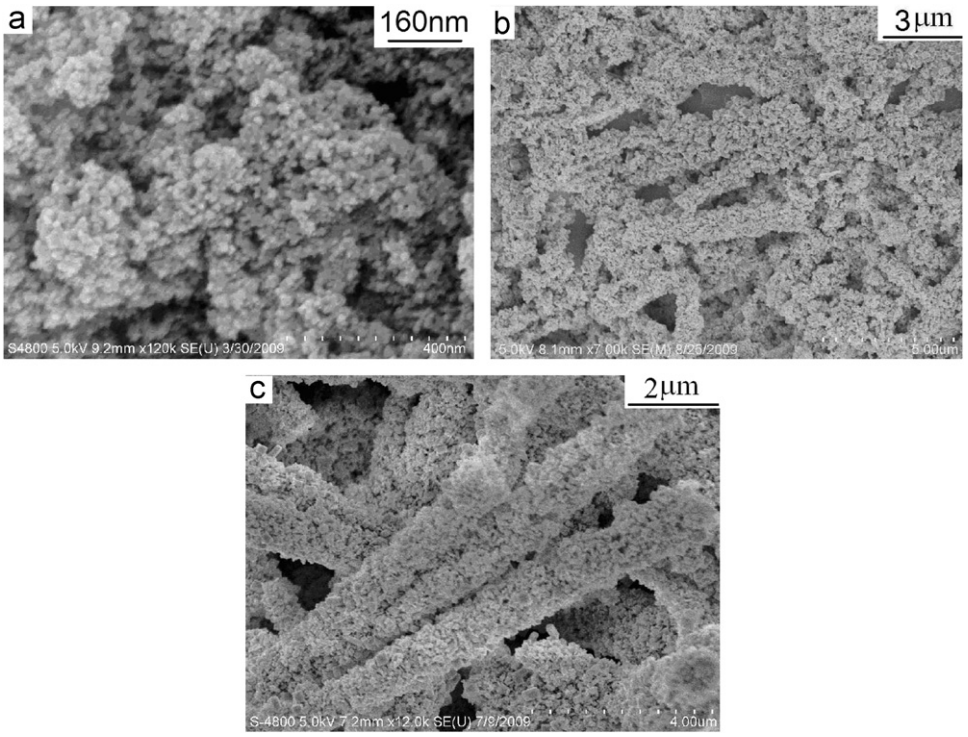

Fig. 4. SEM images of the products obtained with 1.0 g of PVP after different reaction time: (a) 1 h, (b) 4 h and (c) 12 h.

microrods be obtained at this time. Fig. S5 (see Supplementary Content) shows the FT-IR spectrum of the as-prepared $BiFeO_3$ sample and the PVP molecule, respectively. After several washings with deionized water and absolute ethanol, the PVP still exists in the final product, indicating that it has strongly adsorbed onto the surface of building units. The absorption features at 564 cm^{-1} are attributed to the Fe–O stretching and bending vibrations, which are characteristics of the octahedral FeO_6 groups in the perovskite compounds [20,31,32].

In order to monitor the morphological evolution and reveal the possible growth mechanism of the one-dimensional rod-like aggregation, a series of time-dependent experiments were carefully carried out to get an insight into the formation process. When the reaction time is controlled at 1 h, the XRD pattern shows that rhombohedral phase $BiFeO_3$ nanoparticles have appeared accompanying with monoclinic Bi_2O_3 and tetragonal Fe_2O_3 (Figs. 4 and 5a). Prolonging the reaction time to 4 h, nanoparticles-assembled BFO microrods appear (Fig. 4b). However, the corresponding XRD pattern shows that monoclinic Bi_2O_3 and tetragonal Fe_2O_3 still exist (Fig. 5b). Careful observations reveal that the peaks of BFO become stronger and the impurities phase have a tendency to disappear. Further prolonging the reaction time to 6 h leads to the harvest of many such rod-like aggregations (Figs. 1a and 2). At 12 h, the morphology and phase of the product preserve (Figs. 4 and 5c).

Based on the above experimental results, a possible formation mechanism of nanoparticles-assembled BFO microrods is proposed. Firstly, the Bi^{3+} and Fe^{3+} cations react with NaOH to form Bi_2O_3 and Fe_2O_3 under solvothermal condition. The following occurrence can be ascribed to the well-known dissolution and reprecipitation process, which has already been demonstrated in the formation of micro/nanostructures by some research groups [33–36]. For example, Zhang et al. [36] reported a general nonaqueous route for the synthesis of phase-pure $InNbO_4$ nanocrystals based on the one-pot solvothermal reaction of niobium chloride and indium acetylacetonate in benzyl alcohol.

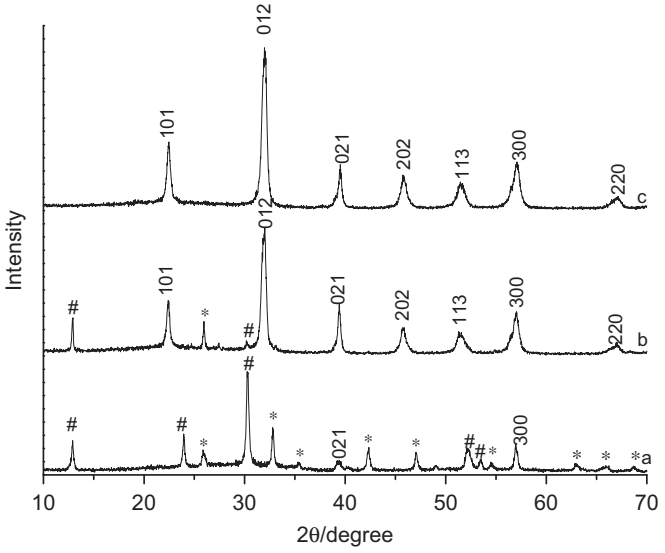

Fig. 5. The XRD patterns of the products obtained with 1.0 g of PVP after different reaction time: (a) 1 h, (b) 4 h and (c) 12 h. (#:Fe_2O_3 15-0615 and ∗:Bi_2O_3 76-1730).

They considered that amorphous niobium oxide particles could be firstly produced in the reaction system. With the prolonging of reaction time, these particles gradually dissolve in benzyl alcohol to form niobium hydroxyl species, which instantly react with $In(OH)_3$ at the surface to produce $InNbO_4$ nuclei. Further growth is then promoted by the higher thermodynamic stability of $InNbO_4$. In our reaction system, similar process may also occur. Under high concentrations of NaOH and high reaction temperature, the initially formed Bi_2O_3 and Fe_2O_3 nanoparticles slowly dissolve to form the corresponding hydroxyl species and further react mutually to the production of BFO nuclei. At the same time, PVP molecules can adsorb one or more suspended solid particles by

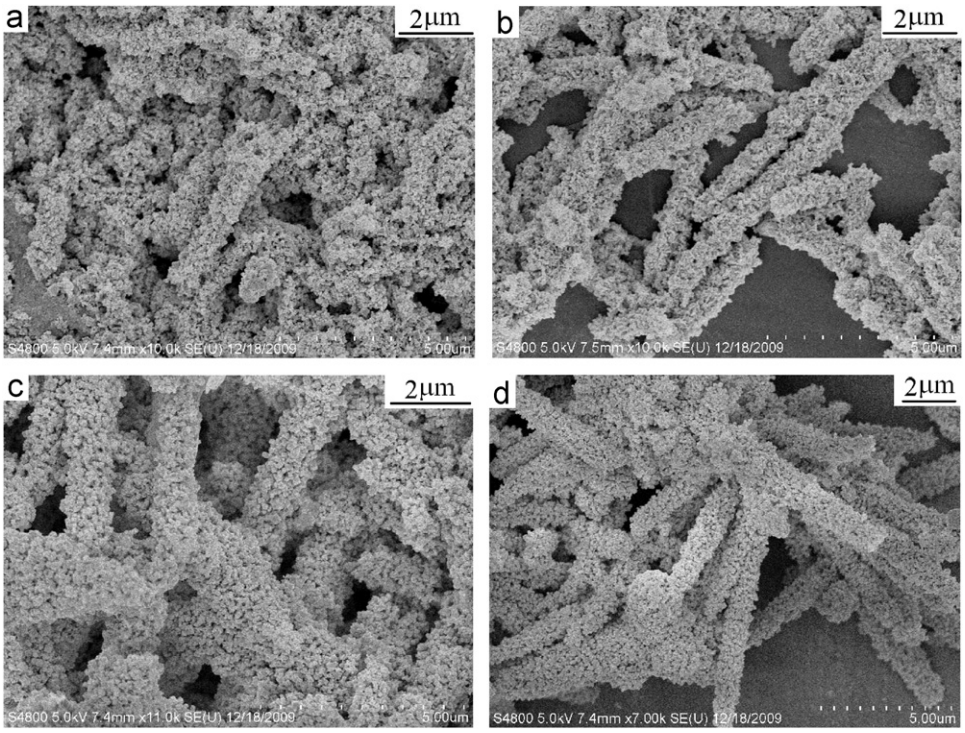

Fig. 6. SEM images of the products with different polymers: (a) 1.0 g of PEG-2000, (b) 1.0 g of PEG-6000, (c) 1.0 g of PEG-10000 and (d) 1.0 g of PEG-20000.

means of their donor groups. The interactions such as the van der Waals force between the polymer molecules adsorbed on the surface of nanoparticles may link these building units together and lead to the formation of nanoparticle-assembled structures. The polymer molecule serves as a middle bridge in such self-assembly process. Wang et al. [37] have already demonstrated that the self-assembly of surfactant-coated nanoparticles was induced by surfactant-modified interparticle interactions and one-dimensional chain arrays of nanoparticles usually occur first as a stable product. Therefore, it is reasonable to assume that such linking effect originated from the interaction between polymer molecules can also result in the attraction of building blocks and favor one-dimensional nanoparticles-assembled BFO microrods as a stable aggregation forms. With the prolonged reaction time, these nanoparticles assemble completely, tightly and the rod-like structures grow longer. Actually, this point is very similar to the polymer-mediated 'bricks and mortar' strategy for the ordering of nanoparticles into structured assemblies proposed by Rotello and co-workers [38–40]. Inorganic nanoparticles correspond to the building brick. The polymer plays as a "mortar" for the self-assembly of nanoparticles due to the strong interaction between the polymer molecules. This suggestion can also be used to explain the effect of the amount of PVP molecules on the rod-like BFO microstructures. At lower concentration of PVP, the "motar" is probably not enough to firmly link such building units. Therefore only BFO nanoparticles were observed in the product. With the appropriate amount of PVP, the microrods based on BFO nanoparticles were completely formed. Such formation mechanism of BFO microrods were further confirmed by the experiments using other linear polymers such as PEG instead of PVP. As shown in Fig. 6 when the PVP is replaced by PEG-2000, PEG-6000, PEG-10000 or PEG-20000, keeping other experimental parameters constant, nanoparticles-assembled rod-like microstructures were also formed. In addition, it should be noted that these assemblies become more tightly with the increasing of the molecular weight of polymer, which can be ascribed to the stronger interaction force of high molecular weight polymer.

The magnetic properties of the nanoparticles-assembled BFO microrods obtained with 1 g of PVP (Fig. 2) and nanoparticles obtained without PVP (Fig. 3a) were studied using the superconducting quantum interference device at room temperature. It is necessary to point out that our microrods were random and the data represent the average of all orientations. As shown in Fig. 7, both BFO microrods and nanoparticles exhibit a weak ferromagnetic order at room temperature, which is quite different from the linear M–H relationship in bulk BFO [41,42]. In fact, this weak ferromagnetic order was also observed in other BFO products, such as film [43] and nanowires [26] and it is suggested that the size effect in nanostructures like films and nanowires may be responsible for the ferromagnetic property [16]. Fig. 7a shows that the saturation magnetizations (M_s) of the BFO microrods and nanoparticles are 0.40 and 0.90 emu g^{-1}, respectively. The coercive force of the former (2025 Oe) is far larger than that of the latter (602 Oe) and the reported values in the literatures (Fig. 7b) [16–18]. In contrast to the isolated nanoparticles, the smaller M_s value of BFO microrods may be related to the presence of PVP molecule, which serves as protective layers on the surface of building blocks. The electron exchange between ligand and surface atoms may quench the magnetic moment and result in the decrease of M_s [44,45]. The remarkable enhancement of coercive force can be ascribed to its unique one-dimensional chain-like structures. It is known that the coercive force of magnetic materials strongly depends on various types of anisotropy (crystal anisotropy, shape anisotropy, stress anisotropy, externally induced anisotropy, and exchange anisotropy), among which the shape anisotropy is predicted to produce the larger coercive forces [46,47].

4. Conclusions

In summary, nanoparticles-assembled one-dimensional $BiFeO_3$ microrods have been successfully prepared via a facile polymer-directed solvothermal route. Experiments indicate that the linking

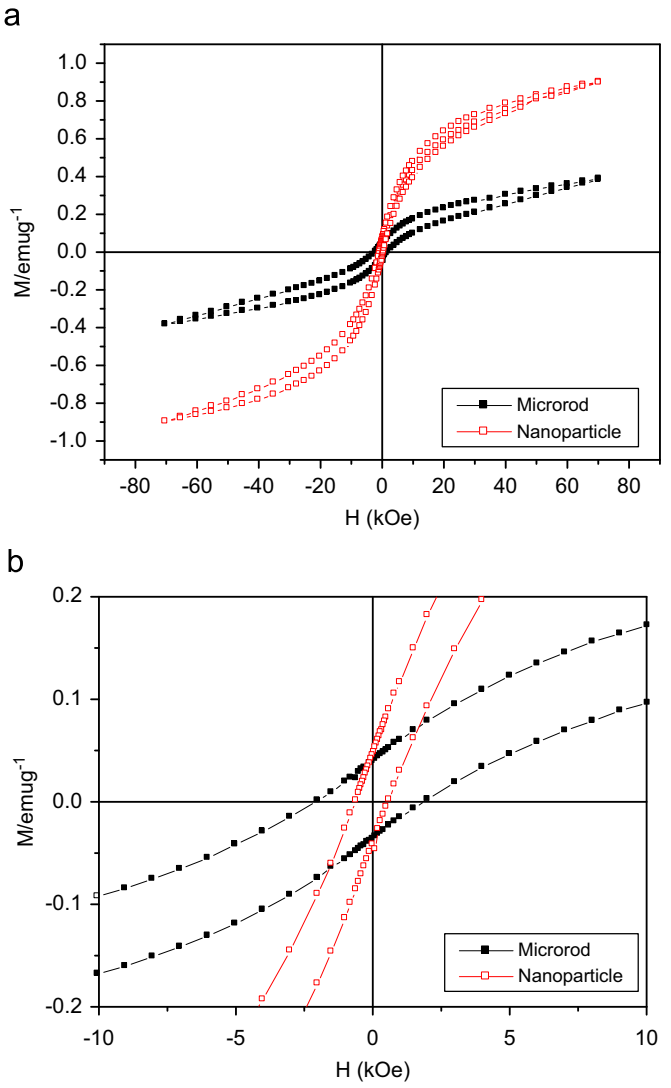

Fig. 7. (a) *M–H* hysteresis loops of BFO microrods obtained with 1 g of PVP and the nanoparticles obtained without PVP measured at room temperature and (b) partially enlarged *M–H* curve of (a).

effect originated from the interactions between polymer molecules can direct the self-assembly of building blocks into the one-dimensional nanoparticles-assembled $BiFeO_3$ microrods as a stable aggregation form. Magnetic properties show that the BFO microrods exhibit smaller saturation magnetizations and larger coercive force than the nanoparticles. Compared to existing preparation routes, the present solvothermal method provides a facile, high-yield, low-cost pathway to novel BFO rod-like nanoarchitectures.

Acknowledgments

This work was supported by the National Basic Research Program of China (Nos. 2006CB806104 and 2007CB925102), Natural Science Grant of China (No. 20721002) and the US National Science Foundation (CHE-0516928).

Appendix A. Supporting Information

Supplementary data associated with this article can be found in the online version at doi:10.1016/j.jssc.2010.05.029.

References

[1] Y.G. Sun, Y.N. Xia, Science 298 (2002) 2176–2179.
[2] X.F. Qian, X.M. Zhang, C. Wang, Y. Xie, Y.T. Qian, Inorg. Chem. 38 (1999) 2621–2623.
[3] V.F. Puntes, K.M. Krishnan, A.P. Alivisatos, Science 291 (2001) 2115–2117.
[4] X.L. Hu, J.C. Yu, Adv. Funct. Mater. 18 (2008) 880–887.
[5] N.N. Zhao, L.M. Qi, Adv. Mater. 18 (2006) 359–362.
[6] Y.W. Jun, J.S. Choi, J.W. Cheon, Angew. Chem. Int. Ed. 45 (2006) 3414–3439.
[7] H.Y. Zhou, S.L. Xiong, L.Z. Wei, B.J. Xi, Y.C. Zhu, Y.T. Qian, Cryst. Growth Des. 9 (2009) 3862–3867.
[8] D.J. Cheng, W.C. Wang, D.P. Cao, S.P. Huang, J. Phys. Chem. C 113 (2009) 3986–3997.
[9] D.K. Ma, X.K. Hu, H.Y. Zhou, J.H. Zhang, Y.T. Qian, J. Cryst. Growth 304 (2007) 163–168.
[10] L. Li, W.G. Jiang, H.H. Pan, X.R. Xu, Y.X. Tang, J.Z. Ming, Z.D. Xu, R.K. Tang, J. Phys. Chem. C 111 (2007) 4111–4115.
[11] J.H. Zeng, J. Yang, Y. Zhu, Y.F. Liu, Y.T. Qian, H.G. Zheng, Chem. Commun. (2001) 1332–1333.
[12] M. Rycenga, P.H.C. Camargo, Y.N. Xia, Soft Matter 5 (2009) 1129–1136.
[13] X.S. Shen, G.Z. Wang, X. Hon, W. Zhu, CrystEngComm 11 (2009) 753–755.
[14] Z.X. Deng, Y. Tian, S.H. Lee, A.E. Ribbe, C.D. Mao, Angew. Chem. Int. Ed. 44 (2005) 3582–3585.
[15] T. Cai, Z.B. Hu, Langmuir 20 (2004) 7355–7359.
[16] F. Gao, X.Y. Chen, K.B. Yin, S. Dong, Z.F. Ren, F. Yuan, T. Yu, Z.G. Zou, J.M. Liu, Adv. Mater. 19 (2007) 2889–2892.
[17] T.J. Park, Y.B. Mao, S.S. Wong, Chem. Commun. (2004) 2708–2709.
[18] T.J. Park, G.C. Papaefthymiou, A.J. Viescas, A.R. Moodenbaugh, S.S. Wong, Nano Lett. 7 (2007) 766–772.
[19] J. Chen, X.R. Xing, A. Watson, W. Wang, R.B. Yu, J.X. Deng, L. Yan, C. Sun, X.B. Chen, Chem. Mater. 19 (2007) 3598–3600.
[20] T. Xian, H. Yang, X. Shen, J.L. Jiang, Z.Q. Wei, W.J. Feng, J. Alloys Compd. 480 (2009) 889–892.
[21] M. Valant, A.K. Axelsson, N. Alford, Chem. Mater. 19 (2007) 5431–5436.
[22] J.K. Kim, S.S. Kim, W.J. Kim, Mater. Lett. 59 (2005) 4006–4009.
[23] J. Wei, D.S. Xue, Mater. Res. Bull. 43 (2008) 3368–3373.
[24] J.H. Xu, H. Ke, D.C. Jia, W. Wang, Y. Zhou, J. Alloys Compd. 472 (2009) 473–477.
[25] S. Farhadi, M. Zaidi, J. Mol. Catal. A: Chem. 299 (2009) 18–25.
[26] F. Gao, Y. Yuan, K.F. Wang, X.Y. Chen, F. Chen, J.M. Liu, Appl. Phys. Lett. 89 (2006) 102506.
[27] T.T. Fang, C.C. Ting, J.H. Miao, J. Am. Ceram. Soc. 92 (2009) 3065–3069.
[28] Y.G. Wang, G. Xu, L.L. Yang, Z.H. Ren, X. Wei, W.J. Weng, P.Y. Du, G. Shen, G.R. Han, Ceram. Int. 35 (2009) 1285–1287.
[29] Y.G. Wang, G. Xu, Z.H. Ren, X. Wei, W.J. Weng, P.Y. Du, G. Shen, G.R. Han, J. Am. Ceram. Soc. 90 (2007) 2615–2617.
[30] S. Li, Y.H. Lin, B.P. Zhang, J.F. Li, C.W. Nan, J. Appl. Phys. 105 (2009) 054310.
[31] W. Kaczmarek, A. Graja, Solid State Commun. 17 (1975) 851–853.
[32] G.V.S. Rao, C.N.R. Rao, J.R. Ferraro, Appl. Spectrosc. 24 (1970) 436–445.
[33] J.C. Yu, L.Z. Zhang, Q. Li, K.W. Kwong, A.W. Xu, J. Lin, Langmuir 19 (2003) 7673–7675.
[34] R.I. Walton, F. Millange, R.I. Smith, T.C. Hansen, D. O'Hare, J. Am. Chem. Soc. 123 (2001) 12547–12555.
[35] W.J. Wang, J.S. Bi, L. Wu, Z.H. Li, X.X. Wang, X.Z. Fu, Nanotechnology 19 (2008) 505705.
[36] L.Z. Zhang, G. Garnweitner, I. Djerdj, M. Antonietti, M. Niederberger, Chem. Asian J. 3 (2008) 746–752.
[37] J.C. Wang, P. Neogi, D. Forciniti, J. Chem. Phys. 125 (2006) 194717.
[38] A.K. Boal, F. Ilhan, J.E. DeRouchey, T. Thurn-Albrecht, T.P. Russell, V.M. Rotello, Nature 404 (2000) 746–748.
[39] A.K. Boal, T.H. Galow, F. Ilhan, V.M. Rotello, Adv. Funct. Mater. 11 (2001) 461–465.
[40] T.H. Galow, U. Drechsler, J.A. Hanson, V.M. Rotello, Chem. Commun. (2002) 1076–1077.
[41] J. Wei, D.S. Xue, Y. Xu, Scripta Mater. 58 (2008) 45–48.
[42] S.T. Zhang, M.H. Lu, D. Wu, Y.F. Chen, N.B. Ming, Appl. Phys. Lett. 87 (2005) 262907.
[43] J. Wang, J.B. Neaton, H. Zheng, V. Nagarajan, S.B. Ogale, B. Liu, D. Viehland, V. Vaithyanathan, D.G. Schlom, U.V. Waghmare, N.A. Spaldin, K.M. Rabe, M. Wuttig, R. Ramesh, Science 299 (2003) 1719–1722.
[44] G.Q. Zhang, T. Zhang, X.L. Lu, W. Wang, J.F. Qu, X.G. Li, J. Phys. Chem. C 111 (2007) 12663–12668.
[45] D.A. Van Leeuwen, L.M. Van Ruitenbeek, L.J. De Jongh, A. Ceriotti, G. Pacchioni, O.D. Haberlen, N. Rosch, Phys. Rev. Lett. 73 (1994) 1432–1435.
[46] L.L. Diandra, D.R. Reuben, Chem. Mater. 8 (1996) 1770–1783.
[47] Z.G. An, S.L. Pan, J.J. Zhang, J. Phys. Chem. C 113 (2009) 1346–1351.